Pol. J. Environ. Stud. Vol. XX, No. X (XXXX), 1-15
DOI: 10.15244/pjoes/187144 ONLINE PUBLICATION DATE:

Original Research

Evaluation of Suitability for Built-Up Land Expansion and Land Use Simulation Based on Obstacle Factor Constraints

Shidong Wang, Jinyin Pan, Li Li*

[1]Henan Polytechnic University (HPU), School of Surveying and Engineering Information, Jiaozuo 454003, China

Received: 31 December 2023
Accepted: 13 April 2024

Abstract

The expansion of built-up areas has a significant impact on the spatial distribution of land use within a given region. The accurate identification of appropriate regions for the expansion of built-up land holds significant importance in shaping the future distribution of land use patterns. Using Sanmenxia City in Henan Province as a case study, this analysis focuses on obstacle factors such as the suitability of land resources, ecological service value, and ecological security. A built-up land expansion suitability evaluation index system was developed, and the weights were determined using entropy gray correlation analysis. We employed the weighted average comprehensive index model to examine the attributes associated with the suitability of built-up land expansion within the designated study region. Subsequently, the PLUS model was employed to simulate the prospective land utilization within the study area, with the suitability of built-up land expansion as a constraint. The findings of this study will serve as a fundamental framework for informing decision-making processes pertaining to land space planning, ecological construction, and urban development in Sanmenxia City.

Keywords: obstacle factors, built-up land expansion, appropriateness, PLUS, land use simulation

Introduction

The expansion of built-up land has become a significant component of land use change due to population growth and socio-economic development [1]. Nevertheless, this transition has also given rise to a myriad of issues, including ecological and environmental damages, heightened land incongruity, supplementary land allocation for construction purposes, and the degradation and contamination of land [2]. The extensive and haphazard expansion of built-up land has resulted in suboptimal land utilization [3]. Therefore, strategic land expansion holds significant importance for promoting efficient land use in the region and for the spatial planning of the entire nation [4].

The assessment of the suitability of expanding built-up land involves a thorough evaluation that considers the natural, social, and economic factors of the city. This evaluation is conducted in accordance with ecological protection and construction requirements [5]. Its purpose is to determine the optimal direction for future expansion of built-up land. The selection of indicators and the determination of weights are crucial steps in

*e-mail: ll_980101@163.com
Tel.: +8618162697600

assessing the suitability of built-up land expansion [6]. In previous research, indicators have predominantly been chosen from the realms of the natural environment and socio-economic circumstances. The inclusion of multiple criteria with varying weights in the evaluation process introduces complexity to the assessment procedure. Various methods can be employed to determine weights, such as factor analysis [7, 8], principal component analysis [9], Analytic Hierarchy Process (AHP) [10, 11], entropy method [12, 13], and gray correlation analysis [14, 15]. The Analytic Hierarchy Process (AHP) is widely acknowledged as a highly effective approach for multi-criteria decision-making. It utilizes a hierarchical structure to depict the relative significance of factors and the relationships within a multi-criteria decision-making framework [16]. Nevertheless, this approach is hindered by its incapacity to address the undisclosed certainty inherent in the decision-making procedure, resulting in imprecise outcomes. The proposed method, known as the entropy method-gray correlation analysis method, offers a more objective approach to calculating assigned weights. This is achieved by substituting the subjective results obtained from the entropy method with the traditional approach of utilizing the value of the discriminant coefficient in gray correlation analysis.

Several established dynamic models have been developed in the field of future land use simulation. These models include logistic regression [17], Markov [9, 10], meta-cellular automata (CA) [18-20], conversion of land use and its effects (CLUE) [21-23], the Future Land Use Simulation (FLUS) model [24, 25], and the Patch Generated Land Use Simulation (PLUS) model [26-29]. The utilization of cellular automaton (CA) models has yielded favorable outcomes in urban area modeling in both local and cross-national investigations. In a study conducted by Li et al. [30], the authors employed a combination of the MCR model and the CA-Markov model to simulate the projected growth of the Wuhan metropolitan area. Their findings indicate that the MCR-modified CA-Markov model holds promise for facilitating environmentally sustainable urban expansion. In their study, Sai Hu et al. [31] employed the gray early warning GM(1,1) model and FLUS model to simulate the anticipated characteristics of land use change in Anhui Province under an ecological optimization scenario. The PLUS model was initially proposed by Xun Liang et al. [32]. This model combines a land expansion analysis strategy with a cellular automaton (CA) model that utilizes various types of stochastic patch seeds. It has the capability to simulate the generation and evolution of multiple types of land patches in a spatio-temporal and dynamic manner. Furthermore, the model can uncover the underlying mechanisms of land use change during the simulation process.

This study focuses on Sanmenxia City as the subject of investigation and assesses the suitability of built-up land expansion by considering constraints related to obstacle factors, drawing upon existing research. The extraction of obstacles to built-up land expansion was conducted based on the natural geography of the study area and the requirements of built-up land development. These obstacles were then categorized into three groups: obstacles related to land resource suitability, obstacles related to ecological service value, and obstacles related to ecological security. The entropy value-gray correlation method is employed to determine the weight of each index for assessing the suitability of expanding built-up land. This allows for the identification of suitable areas for built-up land expansion. Subsequently, the PLUS model is utilized to simulate the prospective land use spatial pattern, taking into account the suitability of expanding built-up land. The findings of this study will serve as a fundamental framework for informing decision-making processes pertaining to land space planning, ecological construction, and urban development in Sanmenxia City.

Overview of the Study Area and Data Sources

Overview of the Study Area

Sanmenxia City is situated in the western region of Henan Province, at the confluence of Henan, Jin, and Shaanxi Provinces. It is positioned between the latitudes of 33°31′24″~35°05′48″N and longitudes of 110°21′42″~112°01′24″E (Fig. 1). The region's topography is characterized by a prevalence of mountains, hills, and the Sichuan Plateau. It spans a land area of 9936.65 km^2, with 5421 km^2 designated as mountainous area, 3250 km^2 as hilly terrain, and 965 km^2 as plains. The area falls within a semi-arid climate, specifically the warm-temperate continental monsoon climate. The average annual temperature is recorded at 14.2°C, and the region typically experiences annual rainfall ranging from 400-700 mm. By the year 2021, it is projected that the overall population of the city will reach 2038 thousand individuals. Among this population, approximately 1182.7 thousand individuals are expected to reside in urban areas, while the remaining 855.3 thousand individuals are anticipated to reside in rural areas. Consequently, the urbanization rate of the resident population is estimated to be 58.03%. The gross domestic product (GDP) of the city amounted to $158.254 billion. The cultivated land area for grain in the city measures 163.93 thousand hm^2. The wheat planting area encompasses 75.17 thousand hm^2, while the corn planting area spans 60.27 thousand hm^2. Additionally, the oilseed planting area covers 13.35 thousand hm^2, and the vegetable planting area extends to 32.85 thousand hm^2. The urban area exhibits a combined yearly grain yield of 730.6 thousand tons, comprising 359.7 thousand tons of summer grain, 370.9 thousand tons of autumn grain, and 40.1 thousand tons of roasted tobacco. The oilseed production amounted to 38.1 thousand tons. The combined production of vegetables and edible fungi

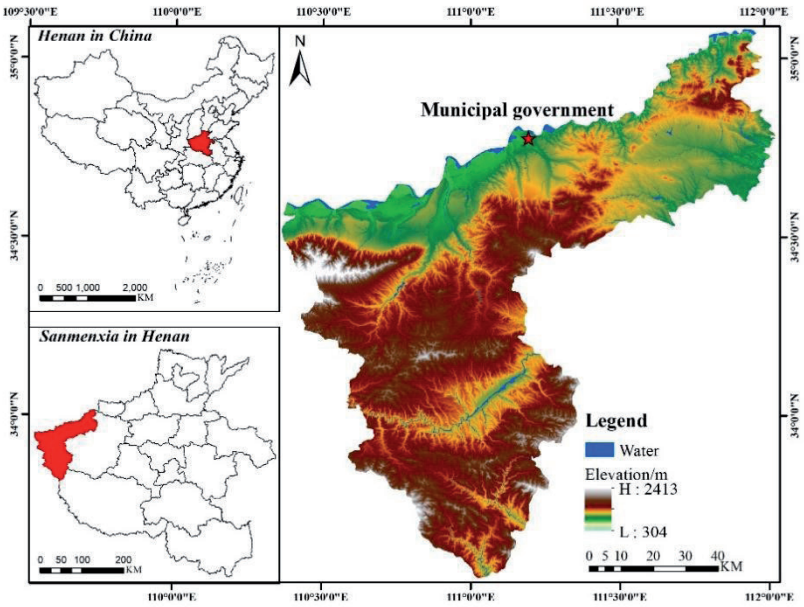

Fig. 1. Geographical location of the study area.

amounts to 1,271,700 tons. The total production of garden fruits amounted to 2682.7 thousand tons.

Data Sources

The dataset used in this study consists of the evaluation indicator system dataset and the driver dataset. The primary datasets encompass land use/land cover data, digital elevation models, meteorological data, and socio-economic data. (1) Raster images of land use in 2010 and 2020 based on the LUCC system reclassified into six categories: cropland, forest land, grass, watershed, built-up land and bare land were provided by the Center for Resource and Environmental Science and Data of the Chinese Academy of Sciences (CRESD); (2) National Aeronautics and Space Administration (NASA) provided 30M resolution digital elevation data and indirectly slope and aspect data; (3) data on railroads and highways was obtained from the National Geographic Information Resources Catalog Service System data; (4) National meteorological science data sharing service platform provided precipitation and temperature data;

Table 1. Source of data for the study area.

Data type	Data name	Year	Source
Raster data	Land use data	2000/2010/2020	https://www.resdc.cn/
	Digital elevation data	2020	https://urs.earthdata.nasa.gov/
	GDP	2019	https://www.resdc.cn/
	Population density data	2020	https://hub.worldpop.org/
	Meteorological data	2020	http://data.cma.cn/
Vector data	Road data	2020	https://www.webmap.cn/
	Water system data	2020	https://data.casearth.cn/
Land use planning data	Sanmenxia City Land Use Master Plan	2000-2020	Sanmenxia Municipal People's Government website, Natural Resources and Planning Bureau website
	Sanmenxia City Master Plan	2013-2030	
Socio-economic data	Sanmenxia Statistical Yearbook	2000-2020	Statistical Yearbook Sharing Platform
	Sanmenxia Statistical Bulletin		Sanmenxia Municipal Government Portal
	China Agricultural Products Price Survey Yearbook	2020	China Agricultural Products Price Survey Yearbook

Table 2. Evaluation index system for suitability of spatial expansion of construction land.

Target level	System level	System level weighting	Indicator layer	Indicator layer weights
Spatial expansion of building land	Obstacles to land resource suitability	0.498	DEM	0.032
			Elevation	0.043
			Distance to water source	0.083
			Distance to highways and railroads	0.162
			Distance from national roads and highways	0.206
			Distance to town	0.041
			Distance to village	0.217
			Distance to address disaster site	0.215
	Obstacles to the value of ecological services	0.165	Support Services	0.375
			Regulatory services	0.250
			Supply service	0.250
			Cultural service	0.125
	Obstacles to ecological security	0.347	NDVI	0.143
			Elevation	0.147
			Population density	0.096
			Land use type	0.098
			Ecological reserve	0.096
			GDP	0.106
			Plaque density	0.089
			Shannonville Index	0.107
			Ecosystem resilience	0.118

(5) The Center for Resource and Environmental Sciences and Data of the Chinese Academy of Sciences (CRESD) provided 2019 GDP data in lieu of 2020 data; (6) The 2000-2020 Statistical Yearbook were used to elivit the data on energy consumption and agricultural resources in Sanmenxia City for the corresponding years; (7) Population data were obtained from the Open Space Population Data (WorldPop). Please refer to Table 1 for further information.

Research Methodology

Evaluation of Suitability for Spatial Expansion of Built-Up Land

The adaptability evaluation of built-up land refers to the process of establishing a scientific and reasonable evaluation system based on the natural, economic, social, and policy conditions of construction land, using scientific methods to determine the most suitable planning use of a certain area or a certain plot of construction land.

Establishment of the Evaluation Indicator System

The prevailing body of research primarily focuses on investigating the factors that contribute to the expansion of built-up land, with particular emphasis on the natural environment and socio-economic data. The examination of obstacle factors associated with the driving force theory pertains to the analysis of factors that hinder the expansion of urban built-up land from an alternative standpoint. This entails investigating the factors that exert an obstructive influence on the development of a specific entity, with each driving factor in the process also being subject to scrutiny as an obstacle factor [33]. When selecting indicators, it is important to consider the principle of combining systematicity and hierarchy, comprehensiveness, and generalization. Incorporating the land's natural resources and the socio-economic status of Sanmenxia City, this research opted for the obstacle factors of land resource suitability, ecological

service value, and ecological security. These factors were utilized to establish the suitability of spatial expansion of built-up land, considering the constraints imposed by the obstacle factors. Subsequently, an indicator system was developed to evaluate this expansion, as depicted in Table 2.

The slope data were acquired from the digital elevation model (DEM) through the utilization of the Slope tool in ArcGIS 10.7. The categorization of ecosystem services into supporting services, regulating services, provisioning services, and cultural services is derived from the ecosystem service valuation system proposed by Costanza et al. [34]. This classification is further informed by the table of equivalent factors for the value of China's terrestrial ecosystem services established by Xie Gao Di et al. [35]. The economic value of a unit of ecosystem services is accurately determined by applying equations (1) and (2) and subsequently revised using equation (3). The calculation of patch density and Shannonville index was performed using Fragstats 4.2 software, utilizing land use classification raster images. The Elastic Ecosystem (ECO) was determined by quantifying land use types using equation (4).

$$ESV = \sum_{i=1}^{n} A_i \times VC \tag{1}$$

$$VC_i = \sum_{i=1}^{n} EC_i \times E_a \tag{2}$$

where *ESV* is ecosystem services value; *i* is the land use type; *j* is the type of ecosystem service; A_i is the area of land use type *i*; VC_i is the value of ecosystem services per unit area of land use type *i*; and EC_i is the equivalent value of ecosystem services for a given land use type.

$$E_a = \frac{1}{7}\sum_{i=1}^{n} \frac{m_i p_i q_i}{M} \tag{3}$$

where E_a is the economic value per unit of ecosystem service; *i* is the type of food crop; m_i is the national average price of the *i*th food crop; and p_i is the yields of the *i*th food crop; E_a is the economic value per unit of ecosystem service; *i* is the type of food crop; m_i is the national average price of the *i*th food crop (yuan/kg); and p_i is the yields of the *i*th food crop.

$$ECO = (0.5 \times S_1 + 0.9 \times S_2 + 0.6 \times S_3 + 0.8 \times S_4 + 0.2 \times S_5 + 0.3 \times S_6)/S \tag{4}$$

where S_1 is the area of cultivated land, S_2 is the area of forested land, S_3 is the area of grass, S_4 is the area of water, S_5 is the area of built-up land, S_6 is the area of unutilized land, and *S* is the total area.

Standardization of Indicators

Indicators can be categorized into positive and negative indicators based on their influence on ecological vulnerability, and these indicators undergo a process of standardization. Positive indicators suggest a positive correlation between the magnitude of the indicator and the severity of ecological degradation and vulnerability. Conversely, negative indicators suggest an inverse relationship, where higher values of the indicator correspond to improved ecological conditions and reduced vulnerability. Based on the inherent characteristics of the evaluation indicators, the indicators exhibiting a positive correlation with vulnerability were subjected to standardization using formula (5), while the indicators displaying a negative correlation with vulnerability were subjected to standardization using formula (6).

$$x_i = \frac{x - x_{min}}{x_{max} - x_{min}} \tag{5}$$

$$x_j = \frac{x_{max} - x}{x_{max} - x_{min}} \tag{6}$$

where is the normalized value of the positive indicator and is the normalized value of the negative indicator.

Entropy Method-Gray Correlation Analysis to Determine Indicator Weights

This study utilizes the concept of gray correlation and its mathematical model to replace the subjective results obtained from the entropy method. Instead, it employs the traditional discrimination coefficient ρ in the gray correlation analysis to calculate the indicator weights in a more objective manner. The entropy method is calculated based on formulas (7)-(9), whereas the weight calculation results are derived by combining formulas (10) and (11).

$$e_j = -k\sum_{i=1}^{n} P_{ij} \ln P_{ij} \tag{7}$$

$$P_{ij} = \frac{x_{ij}}{\sum_{j=1}^{m} x_{ij}} \tag{8}$$

$$w_j = \frac{1 - e_j}{\sum_{i=1}^{n}(1 - e_j)} \tag{9}$$

$$e_{ij} = \frac{min_i\, min_j \left|k_j - x_{ij}\right| + \rho\, max_i\, max_j \left|k_j - x_{ij}\right|}{\left|k_j - x_{ij}\right| + \rho\, max_i\, max_j \left|k_j - x_{ij}\right|} \tag{10}$$

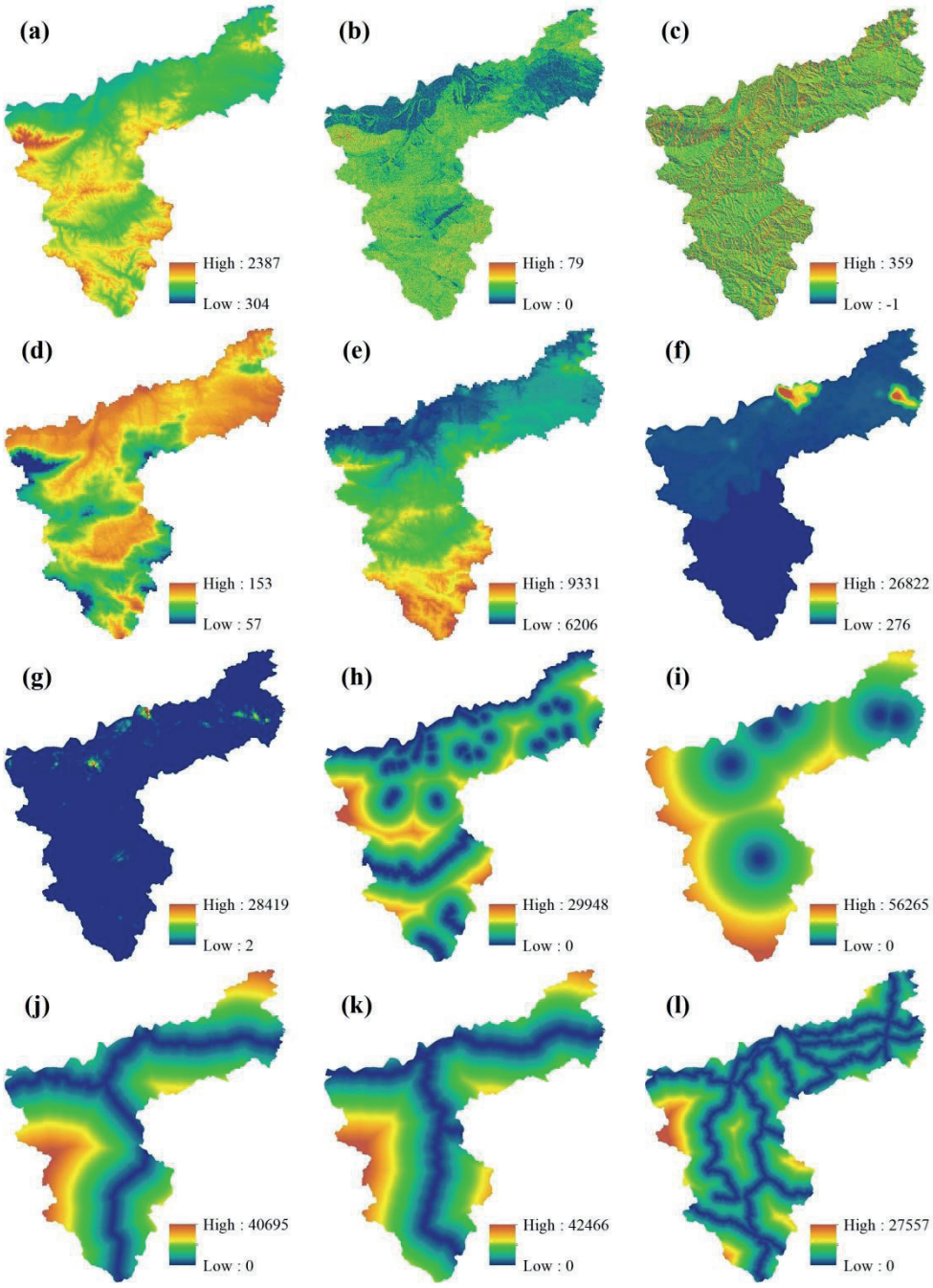

Fig. 2. The main driving factors of land use change in Sanmenxia (a is DEM, b is Slope, c is Aspect, d is Temperature, e is precipitation, f is GDP, g is population density, h is distance to river, i is distance to administrative area, j is distance to railway, k is Distance to high speed, and l is distance to road).

$$w_j = \frac{\frac{1}{n}\sum_{i=1}^{n} e_{ij}}{\sum_{j=1}^{m}\frac{1}{n}\sum_{i=1}^{n} e_{ij}} (j = 1,2,\ldots,m) \tag{11}$$

Where , when , let; ρ is the resolution factor, which takes values in the range of [0,1]; is the minimum difference between two levels; is the maximum difference between the two levels. as the weights of indicators.

Markov Model-Based Land Use Demand Forecasting

The Markov model was employed to forecast the future magnitude of demand for each land use category within the research region. In land use change research, the Markov model is employed to simulate the impact of time phase t on the land use pattern at time phase t+1. The precise computations are illustrated in equation (12):

Table 3. Parameters of domain weights.

Land use type	Cultivated land	Forestry	Grass	Water	Build-up land	Unused land
Domain weighting	0.268	0.351	0.144	0.052	0.177	0.007

$$S_{t+1} = P_{ij} \times S_t \tag{12}$$

where S_t and S_{t+1} denote the state of the land at time-phase t and time-phase $t+1$, respectively; t is the year; P_{ij} is the state transfer probability matrix, which denotes the probability of the transfer of land type i to land type j.

Spatial Simulation of Land Use Based on the PLUS Model

The PLUS model is a novel model built upon metacellular automata, utilizing a novel technique to analyze the expansion of land use, resulting in a more comprehensive understanding of the mechanism behind land use change. The model combines the Land Expansion Analysis Strategy (LEAS) rule mining method with the multi-class random patch seeds (CARS) metacellular automata model, which identifies changes in land use types over two periods and investigates the correlation between these changes and the driving factors using the Random Forest algorithm. The LEAS method was employed to determine the growth probability for each land use category within the research area. This information was then combined with the number of image elements, transformation matrix, and domain weights assigned to distinct land use types. Using the CARS model, these factors were used to simulate the future spatial distribution of land use. The procedure consists of the following steps:

Identification of driving factors: Based on the current conditions of the study area and taking into account relevant research findings, 12 driving factors were chosen. These factors include elevation, slope, slope direction, average annual temperature, average annual precipitation, GDP, population density, proximity to rivers, proximity to administrative centers, proximity to railroads, proximity to highways, and proximity to highways (Fig. 2).

(2) Setting of restrictive areas: The process of determining restrictive areas involves selecting the top 30% of evaluated areas as suitable for built-up land. These areas are further divided into three categories (I, II, and III) using the natural breakpoint method. In ARCGIS 10.7, the areas unsuitable for conversion are assigned a value of 0, while the areas suitable for conversion are assigned a value of 1. These values are used to define the restrictive areas for built-up land (Fig. 4).

(3) Simulation process: The simulation process involves several steps. Firstly, we select land use images from 2010 and 2020. Then, we use the Extract Land Expansion tool to identify the expansion portion of each type of land use between these two periods. Secondly, we combine the land use expansion images with the driving factors and analyze them using the Land Expansion Analysis Strategies (LEAS) module. We use the Random Forest Classification (RFC) method to determine the size of the drivers, the development probability of each land use type, and the degree of influence of each driver on each land use type. Next, we simulate the 2020 land use map using the CA model of multi-class random patch seeds (CARS). Finally, we verify the accuracy of the simulation using the Validation module.

(4) Neighborhood weight parameter setting: The neighborhood weight parameter is determined by calculating the expansion intensity of land use based on the land use images from 2010 and 2020. The values are standardized to a range of 0-1, where a higher value indicates a stronger expansion ability of the land category, the specific neighborhood weight parameters are shown in Table 3.

(5) Accuracy verification: The accuracy verification of the 2020 simulation image and the 2020 real land use image yielded an overall accuracy of 89.42%, a Kappa coefficient of 90.21%, and a FOM value of 0.26. These results indicate that the simulation accuracy is high and it can be reliably used for the 2030 land use simulation.

Land Use Type Transfer Trajectories

Transfer Matrix

The land use type transfer matrix provides an accurate representation of the number of conversions between different land use types during the study period. This matrix is useful for analyzing the quantitative structural characteristics of different types, as well as the direction and quantity of mutual conversions. The mathematical expression for the transfer matrix is shown in equation (13).

$$S = \begin{bmatrix} S_{11} & \cdots & S_{1j} & \cdots & S_{1n} \\ \vdots & \ddots & \vdots & \ddots & \vdots \\ S_{i1} & \cdots & S_{ij} & \cdots & S_{in} \\ \vdots & \ddots & \vdots & \ddots & \vdots \\ S_{n1} & \cdots & S_{nj} & \cdots & S_{nn} \end{bmatrix} \tag{13}$$

where S denotes the transfer matrix during the study period; Sij denotes the area (km²) of the ith land use type converted to the jth type during the study period and n denotes the number of land use types.

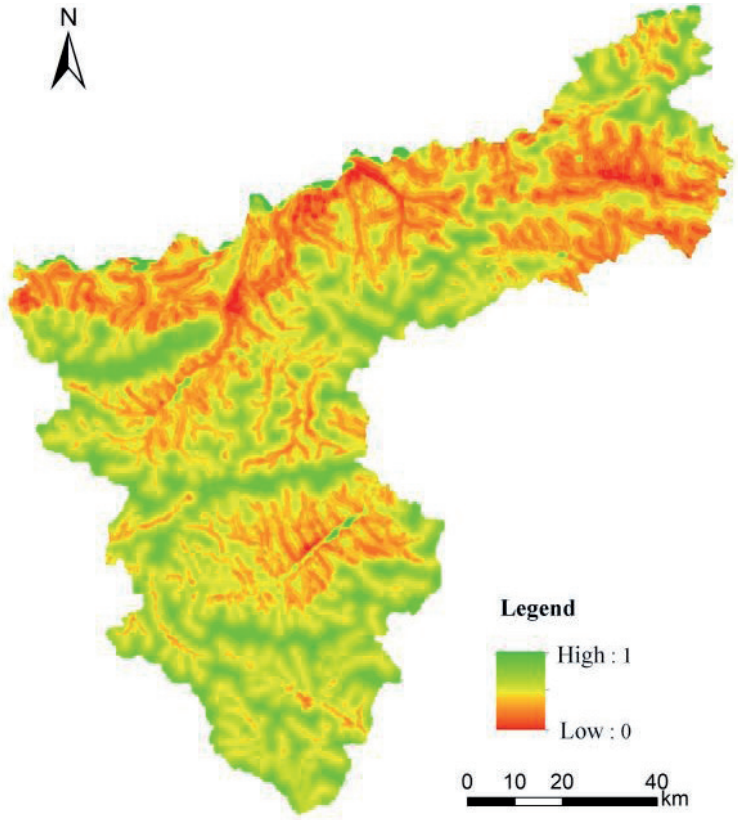

Fig. 3. Evaluation results of suitability for the expansion of built-up land under obstacle factor constraints.

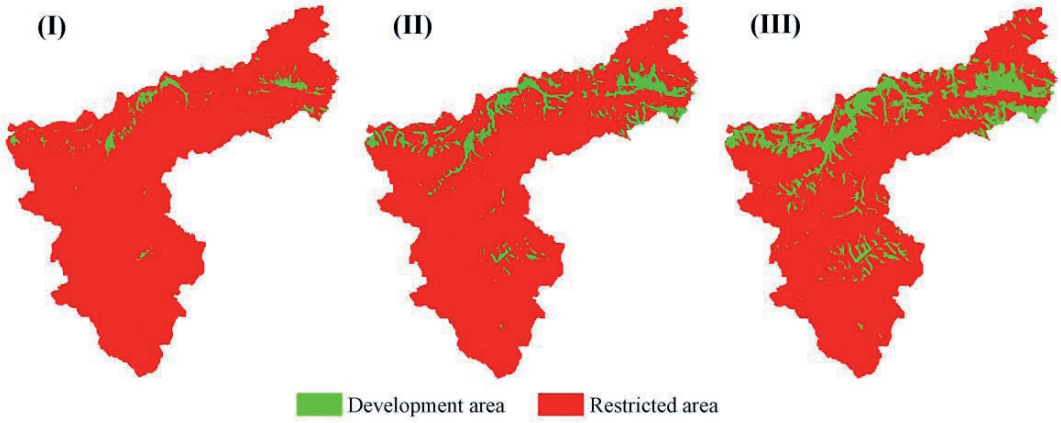

Fig. 4. Suitability of built-up land expansion at three levels.

Inward and Outward Transfer Rates

The transfer-in and transfer-out rates of land use types quantify the proportion of area that is transferred into and out of a specific type, indicating the level of stability of that type during the study period. The transfer-in and transfer-out rates are computed using a transfer matrix, as depicted in equations (14) and (15).

$$Rin_i = \frac{\sum_{i=1}^{n} S_{ij} - S_{ii}}{\sum_{i=1}^{n} S_{ij}} \times 100\% \tag{14}$$

$$Rout_i = \frac{\sum_{j=1}^{n} S_{ij} - S_{ii}}{\sum_{j=1}^{n} S_{ij}} \times 100\% \tag{15}$$

where Rin_i and $Rout_i$ denote the rate of transitions into and out of the ith land use type during the study time period, respectively, and S_{ij} denotes the area of the ith land use type that remained unchanged during the study time period.

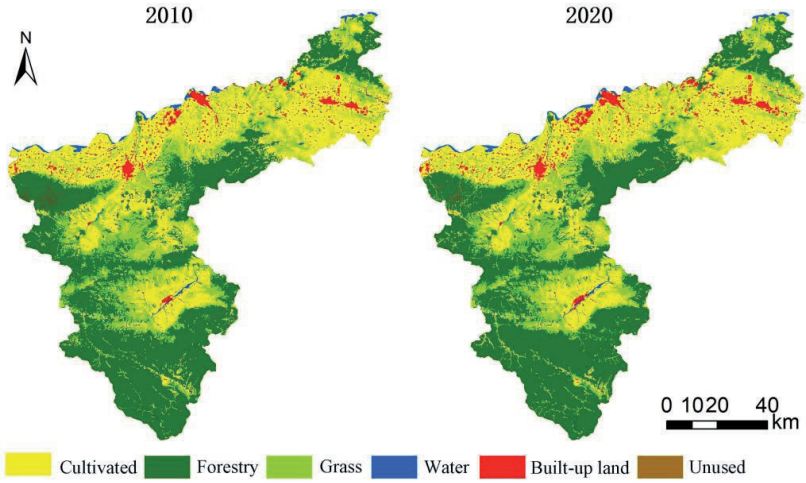

Fig. 5. Land use map of Sanmenxia in 2010 and 2020.

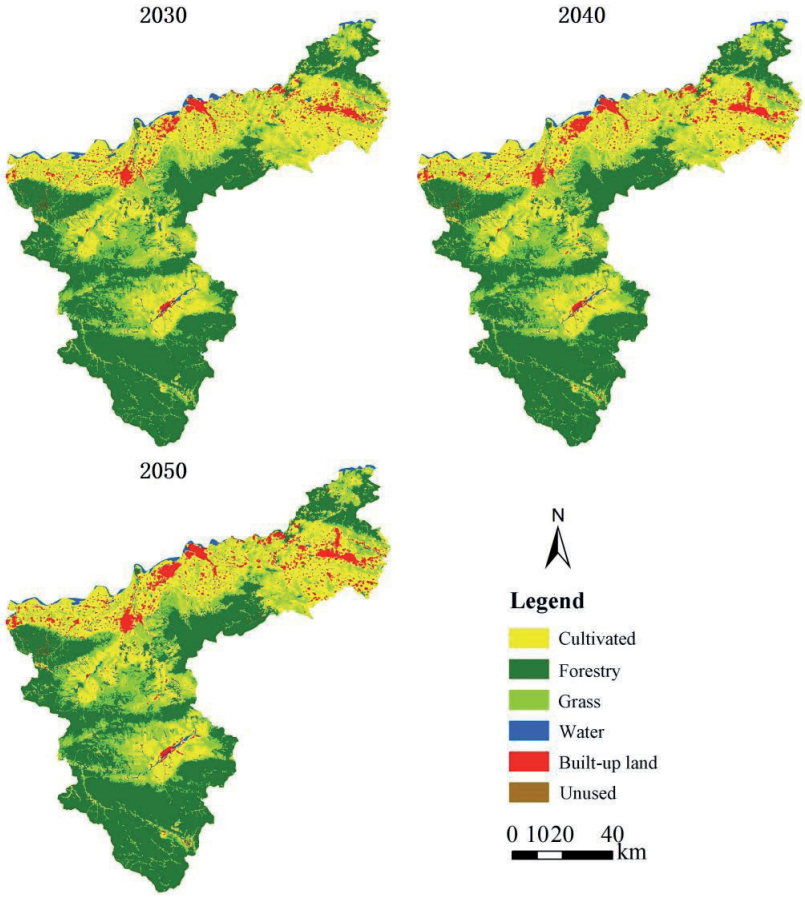

Fig. 6. Land use projection results for Sanmenxia City in 2030, 2040, and 2050.

Results and Analysis

Characteristics of Suitability for Expansion of Construction Land

Based on the findings from the suitability evaluation results of built-up land expansion (as shown in Fig. 3 and Fig. 4), it has been determined that the majority of future build-up land expansion in Sanmenxia City will primarily occur in low-lying and gradually sloping areas. These areas are mainly located in the northern plains near the Yellow River, surrounding the central urban area, and alongside the main roads of the city. The expansions primarily consist of the northeastward growth of Lingbao City along Kaiyuan Avenue, the southeastward growth of Sanmenxia City's central urban

Table 4. Prediction results of land use area.

Type Year	Cultivated land (km²)	Forestry (km²)	Grass (km²)	Water (km²)	Build-up land (km²)	Unused land (km²)
2010	3489.26	4287.79	1665.6	141.34	350.86	1.76
2020	3424.06	4301.38	1637.62	156.18	410.43	4.65
2030	3367.67	4313.80	1611.12	171.05	468.63	4.26
2040	3308.76	4304.77	1641.24	157.44	519.67	4.65
2050	3257.55	4316.49	1629.03	159.07	569.74	4.65

area adjacent to the southwestern Shanzhou District and along the inner side of the Lianhuo Expressway and the Lianxiang Line, and the northward growth of Mianchi County bordering Yima City and along the Hengmian Expressway. The distribution tendency primarily follows an east-west orientation, resulting in a pattern of built-up land development concentrated around the central urban area of Sanmenxia City. This development extends outwards on both sides in a strip expansion fashion.

Characteristics of Future Land Use Simulation Results and Spatial and Temporal Changes

The Markov-PLUS model's accuracy was verified to ensure it met the requirements. Using the land use maps of 2010 and 2020 (Fig. 5), a future land use simulation was conducted. The simulation considered the three-level suitability of build-up land. As a result, the predicted spatial distribution of land use in Sanmenxia City for the years 2030, 2040, and 2050 was obtained (Fig. 6).

Characteristics of Land-Use Area Change

The future quantities of land use in Sanmenxia City were determined using the Markov method (Table 4). The changes in area and annual change rates (Table 5) were then calculated to analyze the quantities and rates of change for different land use types during various time periods from 2010 to 2050. In general, the cultivated land area will progressively decrease annually, while the areas of forestry and unused land will remain stable. The grass area will exhibit some volatility but will stabilize overall. The overall water area will remain stable, save for a little rise in 2030. Conversely, the built-up land area will experience a significant increase. Out of these, the area of cultivated land experienced the most significant reduction, amounting to 231.65km². The pace of change remained relatively constant throughout each decade. Subsequently, grass exhibits a reasonably consistent rate of change for the initial three periods, but will see a substantial fall in 2040-2050 as the trend of decreasing area becomes less pronounced. The built-up land area will experience the most significant expansion, reaching a total of 218.86km². However, its growth rate will reduce from 16.99% to 9.63%, showing a gradual decline in annual growth. The water expanse will experience a gradual and continuous expansion from 2010 to 2030. However, starting in 2030, the pace of this expansion will begin to decrease, eventually dropping to a mere 1.03% by the year 2050. The forest lands will experience a modest shift, with a yearly growth rate of 0.64% between 2010 and 2050.

The transformation of land use types was assessed by computing the rates of transfer in and transfer out, as shown in Table 6. The transfer-out rate of cultivated land is higher than the transfer-in rate from 2010 to 2050, suggesting a consistent decline in the area of cultivated land during this period. Both the transfer-in and transfer-out rates exhibit a decreasing trend, indicating that the decline in cultivated land has been somewhat managed. The rates of transfer-in and transfer-out for woodland are approximately similar, with values ranging from 0.06 to 3.71. These rates predominantly remain at a very low level, suggesting that the size of the forested area will remain largely stable in the future. The transfer-in and transfer-out rate of grass is significantly higher throughout the period of 2010-2030 compared to subsequent years, indicating that a specific area of grass is experiencing instability during this timeframe. However, it is expected to stabilize after 2030. The water in Sanmenxia City experiences a substantial increase from 2010 to 2020, with both the transfer rate and the transfer rate reaching high levels. However, the transfer rate is substantially bigger than the transfer rate, peaking at 15.43%. This indicates a major expansion of the water area in Sanmenxia City during this period. However, between 2030 and 2040, there is a predominant outflow of water, suggesting a decline in the water area to some degree. This trend is expected to stabilize after 2040. The rate of transfer-in for built-up land throughout the period of 2010-2040 is approximately 18%, signifying a significant increase in the expansion of built-up land. However, the growth rate is somewhat regulated after 2040. The transfer rate of unused land reached 65.08% from 2010 to 2020, resulting in a sharp increase in the unused land during this period. With the decrease of the switching-in rate and the increase of the switching-out rate from 2030 to 2040, the area of unused land will begin to decrease and then begin to stabilize after 2040.

Table 5. Amount and annual rate of change of land use area in Sanmenxia City, 2010-2050.

Type	2010-2020		2020-2030		2030-2040		2040-2050		2010-2050	
	Area change (km^2)	Annual change rate (%)	Area change (km^2)	Annual change rate (%)	Area change (km^2)	Annual change rate (%)	Area change (km^2)	Annual change rate (%)	Area change (km^2)	Annual change rate (%)
Cultivated land	-64.98	-1.86	-56.64	-1.65	-58.91	-1.75	-51.20	-1.55	-231.65	-6.64
Forestry	15.22	0.35	9.50	0.22	-9.03	-0.21	11.72	0.27	27.34	0.64
Grass	-27.70	-1.66	-26.65	-1.63	-30.12	-1.87	-12.21	-0.74	-36.39	-2.19
Water	14.93	10.60	15.88	10.26	-13.60	-7.95	1.63	1.03	18.79	13.44
Build-up land	59.64	16.99	58.15	14.17	51.04	10.89	50.07	9.63	218.86	62.39
Unused land	2.90	169.59	-0.24	-5.40	0.39	9.12	0.00	0.00	3.05	191.06

Table 6. Land use transfer rate and transfer out rate in Sanmenxia City, 2010-2050.

Type	2010-2020		2020-2030		2030-2040		2040-2050		2010-2050	
	Rin (%)	Rout (%)	Rin (%)	Rout (%)	Rin (%)	Rout (%)	Rin (%)	Rout (%)	Rin (%)	Rout (%)
Cultivated land	4.26	6.43	3.92	5.84	2.49	4.38	1.50	3.12	5.88	13.80
Forestry	3.71	3.49	1.76	1.57	0.06	0.27	0.35	0.07	4.26	3.78
Grass	5.47	7.57	5.42	7.48	3.32	1.53	2.02	2.83	8.81	12.11
Water	15.43	6.92	15.36	7.15	0.74	9.45	1.10	0.08	18.01	7.52
Build-up land	19.63	6.36	17.21	5.79	18.57	10.75	11.17	2.68	41.68	5.60
Unused land	65.08	6.21	17.57	28.24	8.36	0.00	0.00	0.00	66.82	3.54

Note: Rin represents the transfer rate; Rout represents the turnover rate.

Land-Use Transfer Trajectories

The Sanmenxia City 2010-2050 land use transfer matrix was shown using a Sankey diagram to examine the patterns of land transfer between various categories (Fig. 7). The conversion of cultivated land, forestry, and grass areas achieves a balance of payments between 2010 and 2020. This period experiences the most rapid expansion in unused land, while the conversion of cultivated land and forestry areas leads to an increase in water coverage. From 2020 to 2030, efforts have been made to somewhat mitigate the trend of deforestation and the degradation of forests. Moreover, while the extension of built-up land into agricultural areas has significantly improved, the conversion of cultivated land into water continues to rise, leading to a continuous growth in water areas. Nevertheless, while there is a shift of land from cultivated land areas to grassy areas, the overall cultivated land area is still declining. Between 2030 and 2040, there is a continued increase in built-up land development at the expense of cultivated land. However, the conversion of cultivated land to water is significantly regulated, resulting in a stabilization of water areas on a regional scale. However, during this period, there is an imbalance between the amount of cultivated land and grass, with the conversion of cultivated land to grass being the major trend. The primary source of compensation for cultivated land is derived from built-up land, suggesting that a significant number of illicit and unjustifiable structures were demolished and converted back to cultivated land during this period. The unregulated growth of built-up land has been partially curtailed. Between 2040 and 2050, the increase in developed land has shown the most improvement compared to other years. Additionally, there has been a balance achieved between income and expenditure in cultivated land and grass areas. Furthermore, the tendency of decreasing cultivated land will be well managed throughout this time. The expansion of watersheds and built-up areas reaches a point when it ceases to grow and remains relatively constant. During the period from 2010 to 2050, the predominant occurrence was the significant increase in built-up areas, resulting in the conversion of a substantial portion of fertile land into developed land.

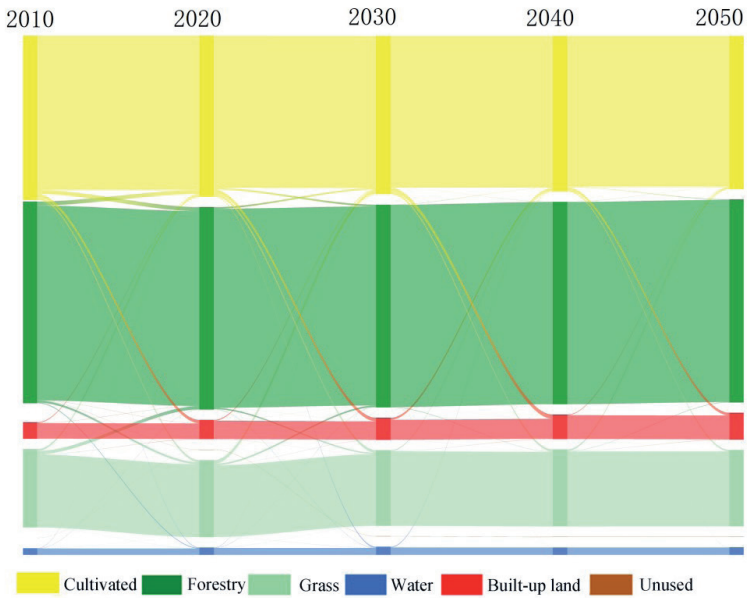

Fig. 7. Land use transfer trajectory in Sanmenxia City, 2010-2050.

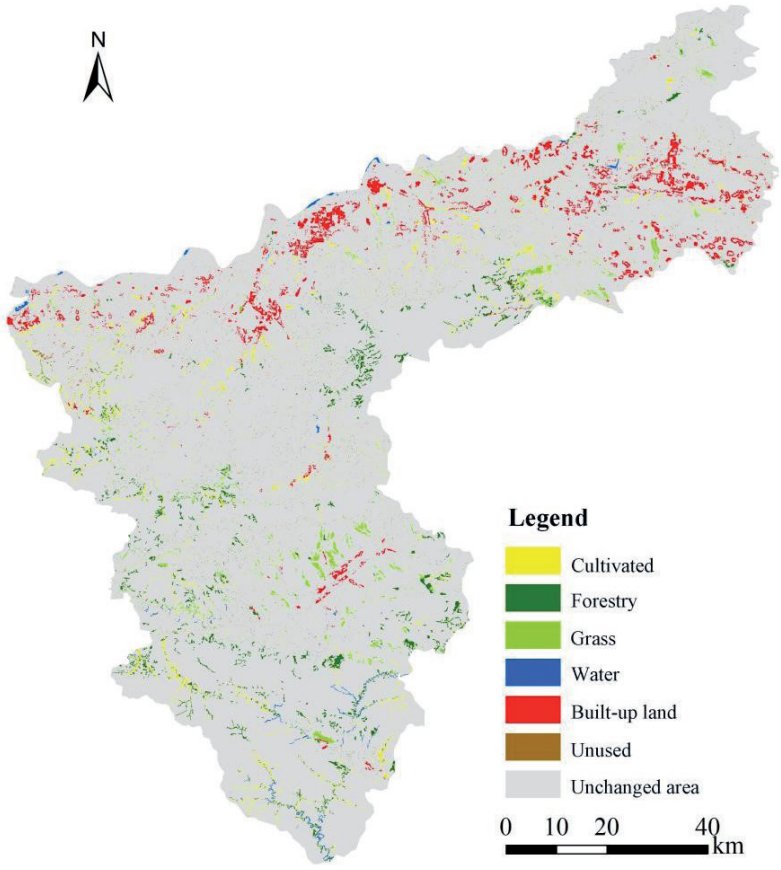

Fig. 8. Land use expansion in Sanmenxia City, 2010-2050.

Characteristics of Land-Use Area Change

Based on the land use spatial pattern in 2010-2050 (Fig. 5 and Fig. 6) and the land use expansion map in 2010-2050 (Fig. 8), it is evident that the rate of land use change in the northern plains is higher during the period of 2010-2050. This suggests that the land use types in this region are relatively dynamic, although the level of activity varies across different time periods. During the period of 2020-2030, the changes in built-up land use

are particularly noticeable, especially when contrasted to changes in other types of land use. These changes primarily occur in the form of expansion around urban areas. The period will witness the primary growth of built-up land in Shanzhou District, with additional clustering of built-up land development in the region. Zhangwan Township, located on the southwest side of Sanmenxia City, will also expand towards Daying Town. Lingbao City will continue to extend upwards along the rivers in the northeastern part of the city. Additionally, Mianchi County and Yima City will continue to share a border and expand northwards along the Hengmian Expressway. The future land use of Sanmenxia City will be planned according to the principles of axial belt development and group layout. The town development space in the Shanling Basin will serve as the primary area for this development. The formation of a belt and group-type town cluster will be based on the Longhai Railway, Lianhuo Expressway, and National Highways 209-310 areas. Additionally, efforts will be made to actively promote the construction of the Mianchi-Yima industrial development wing.

Conclusion and Discussion

This study assesses the suitability evaluation for expansion of built-up land by considering obstacles related to suitability for development, ecological service value, and ecological security. It then uses the results of the built-up land expansion suitability assessment to simulate and predict future land use expansion, treating it as a restricted area for land use development. Finally, it analyzes the characteristics of the changes observed. The primary findings can be summarized as follows:

(1) The majority of the future growth of developed property in Sanmenxia City will mostly consist of low-lying and gradually rising terrain. This land will be located in the northern plains along the Yellow River, as well as in the areas surrounding the center urban area and the main city roadways. The distribution tendency primarily follows an east-west orientation, resulting in a built-up land development pattern centered around the main metropolitan area of Sanmenxia City. This pattern expands in a strip-like manner, expanding outwards on both sides.

(2) From 2010 to 2050, the forestry and unused land area is expected to remain relatively constant. The grass area will fluctuate within a specific range. The water area will generally remain stable, except for a predicted increase in 2030. On the other hand, the cultivated land area will gradually decrease over the 40-year period, with a total reduction of 231.71km². In contrast, the built-up land area will increase by 218.88km², with 90% of it being converted to cultivated land.

(3) Between 2010 and 2050, the rate of land use change in the northern plains zone is very high, with land use types exhibiting quite high levels of activity. Future built-up development will primarily occur in Shanzhou District, with an additional concentration of built-up land in the region. Zhangwan Township, located southwest of Sanmenxia City, will also extend towards Daying Town. Lingbao City will continue to expand along the rivers in the northeastern part of the country. Mianchi County and Yima City will continue to share a border and expand northward along the Hengmian Expressway.

This study establishes the appropriate region for the expansion of built-up land in Sanmenxia City and predicts the future spatial distribution of land use based on this. The findings serve as a valuable guide for the expansion of built-up land and the efficient utilization of land in the area. Nevertheless, there are certain limitations: 1) When constructing the index system to assess the suitability of expanding built-up land, obstacle factors are primarily chosen based on land suitability, ecological value, and ecological safety. However, the selection of obstacle factors does not take into account the connection between built-up land expansion and landscape ecology. In order to more accurately evaluate the appropriateness of developed land, it is necessary to give further consideration to a range of issues in the future. 2) The simulation of future land use only considers the constraint of the suitable area for built-up land expansion, but does not take into account the "three lines". As a result, the future land use outcomes may diverge from the policy planning to some extent. In order to get more accurate outcomes in the future, it is imperative to thoroughly take into account the policy considerations.

Acknowledgements

This work supported by the State Key Project of National Natural Science Foundation of China-Key projects of joint fund for regional innovation and development (U22A20620、U21A20108), Scientific and Technological Innovation Team of Universities in Henan Province（grant number 22IRTSTHN008）. We also want to express our respect and thanks to the anonymous reviewers and the editors for their helpful comments in improving the quality of this paper.

Conflict of Interest

The authors declare no conflict of interest.

References

1. LIU Y.B., HOU X.Y., LI X.W., SONG B.Y., WANG C. Assessing and predicting changes in ecosystem service values based on land use/cover change in the Bohai Rim coastal zone. Ecological Indicators, **111**, 106004, **2020**.
2. YI D., GUO X., HAN Y., GUO J., OU M.H., ZHAO X.M. Coupling Ecological Security Pattern Establishment and Construction Land Expansion Simulation for

Urban Growth Boundary Delineation: Framework and Application. Land, **11** (3), 359, **2022**.
3. ZHANG J.F., WANG C.G., XU L., WENG Y.W. Spatial Effect of Construction Land Misallocation in China:An Empirical Analysis Based on Data of 235 Cities. Tropical Geography, **41** (2), 217, **2021**.
4. ZHU Q.Y., CHEN Y.R., HU W.Y., MEI Y. Spatiotemporal pattern of coupling coordination degree between land intensive use and regional ecological efficiency in China. Transactions of the Chinese Society of Agricultural Engineering, **36** (4), 234, **2020**.
5. XIANG G.G., FU J.H., ZENG L.T., JIANG X.X., ZENG Y. Demarcation technology of urban development boundary based on evaluation of carrying capacity of resourcesenvironment and suitability of land space development: A case study of the central city of Xiangtan county. Journal of Natural Resources, **35** (10), 2401, **2020**.
6. USTAOGLU E., AYDINOGLU A.C. Suitability evaluation of urban construction land in Pendik district of Istanbul, Turkey. Land Use Policy, **99**, 104783, **2020**.
7. ZHAO H.H., CHEN C., GAO S.F. Evaluation of Urban Land Intensive Use and Analysis of lts Driving Factors. Journal of Southwestern University (Natural Science Edition), **41** (5), 112, **2019**.
8. QU C.X, LIU L., FENG X.D. Urban land intensive utilization evaluation and driving factors analysis: Based on Suihua for example. Journal of Northeast Agricultural University, **46** (4), 94, **2015**.
9. BAO Y., HU Z.Q., BAO Y., GUO R.S. Application of principal component analysis and cluster analysis to evaluating ecological safety of land use. Journal of Agricultural Engineering, (8), 87, **2006**.
10. MORALES J.F., VRIES W.T. Establishment of land use suitability mapping criteria using analytic hierarchy process (AHP) with practitioners and beneficiaries. Land, **10** (3), 235, **2021**.
11. BAGHERI M., ZAITION I.Z., MANSOR S. Land-Use Suitability Assessment Using Delphi and Analytical Hierarchy Process (D-AHP) Hybrid Model for Coastal City Management: Kuala Terengganu, Peninsular Malaysia. ISPRS International Journal of Geo-Information, **10** (9), 621, **2021**.
12. ZHAO L., ZHU Y.M., FU M.C., ZHANG P.T., CAO Y.G. Comparative study on intensive use of rural residential land based on principal component analysis and entropy method. Journal of Agricultural Engineering, **28** (7), 235, **2012**.
13. FU Y.H., ZHOU T.T., YAO Y.Y., QIU A., WEI F.Q., LIU J.Q., LIU T. Evaluating efficiency and order of urban land use structure: An empirical study of cities in Jiangsu, China. Journal of Cleaner Production, **283**, 124638, **2021**.
14. ZHAO X., YE J.P., XUE S. Evaluation of sustainable urban land use in Hunan Province based on improved gray correlation analysis. Soil and Water Conservation Bulletin, **33** (3), 265, **2013**.
15. ZHANG Y., LI Q., TU W, MAI K., CHEN Y. Functional urban land use recognition integrating multi-source geospatial data and cross-correlations. Computers, Environment and Urban Systems, **78**, 101374, **2019**.
16. SANTOSH C., KRISHNAIAH C., DESHBHANDARI P.G. Site suitability analysis for urban development using GIS based multicriteria evaluation technique: a case study in Chikodi Taluk, Belagavi District, Karnataka, India// IOP Conference Series: Earth and Environmental Science. IOP Publishing, **169** (1), 012017, **2018**.
17. PENG K., JIANG W., DENG Y. Simulating urban land-use changes by incorporating logistic regression and CLUE-S model: a case study of Wuhan city//2021 28th International Conference on Geoinformatics. IEEE, 1, **2021**.
18. MALTHODI B., KENABATHO P.K., PARIDA B.P., MAPHANYANE J.G. Analysis of the future land use land cover changes in the gaborone dam catchment using ca-markov model: Implications on water resources. Remote Sensing, **13** (13), 2427, **2021**.
19. RAHNAMA M.R. Forecasting land-use changes in Mashhad Metropolitan area using Cellular Automata and Markov chain model for 2016-2030. Sustainable Cities and Society, **64**, 102548, **2021**.
20. ZHAO X., MIAO C. Spatial-Temporal Changes and Simulation of Land Use in Metropolitan Areas: A Case of the Zhengzhou Metropolitan Area, China. International Journal of Environmental Research and Public Health, **19** (21), 14089, **2022**.
21. GU H.L., MA T.J., QIAN F.K., CAI Y.M. County land use scenario simulation and carbon emission effect analysis using CLUE-S model. Journal of Agricultural Engineering, **38** (9), 288, **2022**.
22. AGARWAL C., GREEN G.M., GROVE J.M., EVANS T.P., SCHWEIK C.M. Simulation and Prediction of the Spatial Dynamics of Land Use Changes Modelling Through CLUE-S in the Southeastern Region of Bangladesh. Journal of the Indian Society of Remote Sensing, **49** (11), 2755, **2021**.
23. CHANG X.Y., ZHANG F., CONG K.L., LIU X.J. Scenario simulation of land use and land cover change in mining area. Scientific Reports, **11** (1), 1, **2021**.
24. YUAN X.S., ZHOU J., HU B.B., GAO Q. Multi-scenario simulation and prediction of ecological-productive-living spaces in Guangdong-Hong Kong-Macao Greater Bay Area based on FLUS model. Geoscience, **43** (3), 564, **2023**.
25. CHEN Z., HUANG M., ZHU D., ALTAN O. Integrating remote sensing and a markov-FLUS model to simulate future land use changes in Hokkaido, Japan. Remote Sensing, **13** (13), 2621, **2021**.
26. GAO L., TAO F., LIU R., WANG Z.L., LENG H.J., ZHOU T. Multi-scenario simulation and ecological risk analysis of land use based on the PLUS model: A case study of Nanjing. Sustainable Cities and Society, **85**, 104055, **2022**.
27. ZHAO J.Y.,CUI L.,WANG J., CHEN S. Multi-scenario simulation of urban green space development and construction Timeline based on PLUS model analysis: A case study of the central Zhanjiang City. Journal of Ecology, (18), 1, **2023**.
28. LI L., CHEN Z., WANG S. Optimization of Spatial Land Use Patterns with Low Carbon Target: A Case Study of Sanmenxia, China. International Journal of Environmental Research and Public Health, **19** (21), 14178, **2022**.
29. XU L., GUO W., JIA J. Simulation and Analysis of Land Use Change in Jianghuai Hilly Area Based on PLUS Model. Polish Journal of Environmental Studies, **33** (2), 1899, **2024**.
30. LI X.Q., WANG M.Z., LIU X.J., CHEN Z., WEI X.J.,CHE W.T. Mcr-modified ca–markov model for the simulation of urban expansion. Sustainability, **10** (9), 3116, **2018**.
31. HU S., CHEN L.Q., LI L., ZHANG T., YANG L.N., CHENG L., WANG J., WEN M.X. Simulation of land use change and ecosystem service value dynamics under ecological constraints in Anhui Province, China. International Journal of Environmental Research and Public Health, **17** (12), 4228, **2020**.

32. LIANG X., GUAN Q., CLARKE K.C. Understanding the drivers of sustainable land expansion using a patch-generating land use simulation (PLUS) model: A case study in Wuhan, China. Computers, Environment and Urban Systems, **85**, 101569, **2021**.
33. CHEN D.B., YUE J.W., DING K.S. Land Use Development Based on Fuzzy Comprehensive Evaluation for Multi-Obstacle Factor Construction Land Use. Journal of Subtropical Resources and Environment, **12** (2), 6, **2017**.
34. ROBERT C., RUDOLF G., PAUL S., SANDER V.D.P., SHAROLYN J.A., IDA K., STEPHEN F., KERRY T. Changes in the global value of ecosystem services. Global environmental change, **26**, 152, **2014**.
35. XIE G.D., ZHANG C.X., ZHANG L.M., CHEN W.H., LI S.M. Improvement of the Evaluation Method for Ecosystem Service Value Based on Per Unit Area. Journal of Natural Resources, **30** (8), 1243, **2015**.